AIP | Journal of Applied Physics

Development of crystalline magnetic thin films for microlevitation

Caglar Elbuken, Mustafa Yavuz, and Mir Behrad Khamesee

Citation: Journal of Applied Physics **104**, 044905 (2008); doi: 10.1063/1.2969832
View online: http://dx.doi.org/10.1063/1.2969832
View Table of Contents: http://scitation.aip.org/content/aip/journal/jap/104/4?ver=pdfcov
Published by the AIP Publishing

Development of crystalline magnetic thin films for microlevitation

Caglar Elbuken,[a] Mustafa Yavuz,[b] and Mir Behrad Khamesee[c]
Department of Mechanical and Mechatronics Engineering, University of Waterloo, Waterloo, N2L 3G1 Ontario, Canada

(Received 8 March 2008; accepted 18 June 2008; published online 27 August 2008)

In recent years, magnetic levitation is finding interesting applications in various fields related to microdevices. Producing inexpensive microfabricated magnetic films is of high importance to all magnetically levitated microdevices. This paper introduces a microlevitation system and presents the fabrication of Co–Ni–Mn–P films using electrodeposition. The fabrication parameters are varied such that magnetization direction of the film is varied by changing the crystal structure. The magnetic properties of the films such as coercivity, remanence, and maximum energy product demonstrate that hexagonal structure promotes out-of-plane magnetization whereas cubic structure reinforces in-plane magnetization. The performance of the Co–Ni–Mn–P films is evaluated by magnetic levitation experiments of silicon samples. Satisfactory results are obtained toward the goal of realization of a magnetically levitated microgripper. © *2008 American Institute of Physics*. [DOI: 10.1063/1.2969832]

I. INTRODUCTION

Magnetic levitation is a key technology that provides unique features not only for levitation of massive systems but also for microscale mechanisms. First, using magnetic fields allows noncontact positioning of objects; therefore, eliminates surface friction, which is a big hurdle in microdomain. Second, magnetic levitation systems operate in a completely dust-free manner, which is another asset for microelectromechanical systems (MEMSs). Additionally, the elimination of power or actuation cables promotes the active working domain of the levitated structure. Therefore, in recent years, magnetically levitated microdevices found many applications such as micromotors,[1] microsensors,[2] micropositioning stages,[3] and microrobots.[4]

One requirement for magnetically levitated microsystems is that the system itself should carry a strong magnet to interact with the external magnetic field and form the levitating force. For conventional large-scale systems, commercially available magnets such as NdFeB and SmCo can be used. However, for microsystems, production, handling, and attachment of microscale commercial magnets are practically and financially very challenging. Therefore, there is a great need for cost-efficient methods that can produce strong magnetic materials integrated with the microsystem. Additionally, the magnetization direction of the manufactured magnet should be controlled so that the orientation of the levitating device, a microrobot for instance, can be precisely adjusted. As most of the microsystems are two-dimensional (2D) structures, magnetic films can replace the commercial three-dimensional (3D) magnets for the proposed levitating microdevices. This paper presents a cost-effective and flexible way of producing magnetic films with desired magnetization direction together with the applications of these films.

[a]Electronic mail: celbuken@uwaterloo.ca.
[b]Electronic mail: myavuz@uwaterloo.ca.
[c]Corresponding author. Electronic mail: khamesee@uwaterloo.ca. URL: http://mme.uwaterloo.ca/khamesee.

In order to produce magnetic films, electrodeposition is very promising among many available deposition technologies such as sputtering, spin coating, and screen printing since it provides a good compromise in various aspects. Electrodeposition is a very cost-effective room temperature process enabling relatively fast deposition and high thickness of films.[5] It provides excellent shape fidelity and allows easy tailoring of film properties. The other high temperature fabrication techniques can damage the rest of the microdevice during the deposition of magnetic layer. On the other hand, electrodeposition can be easily integrated in the fabrication cycle of a complex device and reveals the problems associated with fabrication compatibility.

Literature reports that cobalt (Co)-based alloys have satisfactory magnetic properties.[6–9] These alloys such as Co–P, Co–Pt, Co–Ni, Co–Pt–P, Co–Ni–P, Co–Mn–P, and Co–Ni–Mn–P can be easily electrodeposited from aqueous solutions.[10–12] Myung *et al.*[6] provided a comparison of magnetic properties of Co-based hard magnetic alloys. It was revealed that Co-*X*-P (*X*=Ni, Mn, Pt, Ni–Mn)-type alloys have been proven far superior in providing the highest in-plane (horizontal) and out-of-plane (vertical) magnetization values. Among these alloys, it was observed that Co–Ni–Mn–P films can preserve their magnetic properties up to tens of micrometer thickness whereas others deteriorate as the thickness of the film increases.[6] Therefore, Co–Ni–Mn–P alloy is commonly preferred for many applications.

Microlevitation requires the magnetic thin film to be magnetized in a certain direction, in-plane or out-of-plane depending on the design. Thus, magnetization should be enhanced specifically in that direction. It is well known that electrodeposition parameters affect the quality and magnetization direction of the deposited film.[13–16] However, the traditional approach of relating magnetic properties directly to deposition parameters might be misleading because of the cross correlation between all process parameters. Therefore, as Armyanov[17] suggested, determining first the effect of deposition parameters on structural parameters (phase com-

TABLE I. Electroplating bath composition of Co–Ni–Mn–P films.

Compound	g/l
$CoCl_2.6H_2O$	4–24
$NiCl_2.6H_2O$	24
$MnSO_4.H_2O$	3.6
$NaH_2PO_2.xH_2O$	4.6
Saccharin	1
Sodium lauryl sulfate	0.2
NaCl	22
$B(OH)_3$	22

position, crystallinity, texture, and grain size) and then correlating structural properties to magnetic properties provide a better way of analysis. To date, no studies have been presented related to the influence of different crystal structures of Co–Ni–Mn–P films on their magnetic properties. This study also investigates the influence of film crystal structure on the magnetic properties of Co–Ni–Mn–P thin films. We have demonstrated how to improve magnetization in a certain direction by simply modifying the process parameters and changing the crystal structure of the film. Then, various examples of applications of magnetic films are given and finally magnetic levitation of Co–Ni–Mn–P thin film samples is presented. The magnetic levitation setup is described and the experimental verification of levitation of magnetic film coated silicon samples is provided.

II. FABRICATION AND CHARACTERIZATION

Silicon was used as substrate for Co–Ni–Mn–P thin films. 4 in. (100) silicon wafers were RCA-1, 2 cleaned to remove organic residues from the wafers. A 30 nm thick adhesion layer of chromium was deposited by *e*-beam evaporation followed by dc sputtering of 300 nm thick copper seed layer. The wafers were then diced into 5×5 mm^2 pieces for electrodeposition. Using small samples instead of the whole wafers allowed us a better positioning of the anode and cathode to obtain uniform deposits on the substrate.

The composition of electroplating solution was adapted from Cho and Ahn[18] as a basis for our experiments. The weight of bath components for a solution of one liter is summarized in Table I. The first four compounds in the list serve as the source of Co, Ni, Mn, and P ions for the deposit, respectively. Saccharin (or o-benzoic sulfimide) was added as a stress reducer to increase surface activity and hinder passive film formation. Sodium lauryl sulfate was added as a wetting agent to minimize hydrogen pitting, which causes corrosion on film surface. Conductivity and *p*H of the solution were adjusted by the addition of nonreducible cations. A cobalt strip of $50\times5\times1$ mm^3 was used as anode metal to replace depleting Co ions in the bath and to prevent oxidation of hypophosphite.

The deposition was performed at room temperature with a *p*H level of 3.5 for all samples. The interelectrode distance was kept constant at 7 cm. Electrolyte composition, current density, and bath stirring were selected as the parameters to be varied to tailor film properties. Cobalt chloride concentration of the electrolyte was varied between 4 and 24 g/l to observe its effect on the ratio of Co to Ni in the deposited alloy. A dc current density between 3 and 8 mA/cm^2 was applied. Continuous agitation of the bath was achieved by nitrogen pumping for selected depositions.

Scanning electron microscopy (SEM) combined with energy dispersive x-ray spectroscopy was used to measure the local elemental composition of the deposits. Magnetic properties of the films were determined by hysteresis loop measurements performed by a magnetic property measurement system. The surface structure and cross-sectional views were investigated by SEM. X-ray diffraction (XRD) was used to determine the crystal structure. The spectra were obtained with a Cu $K\alpha$ x-ray radiation of 0.154 nm wavelength and 0.2 mm radius collimator. The exposure time was set to 480 s and diffraction angles between 35° and 115° were spanned with 0.02° increments.

III. RESULTS AND DISCUSSION

A. Film composition

Co–Ni–Mn–P thin films are reported to show hexagonal structure with preferably the *c*-axis orientation parallel to film surface normal.[7] However, the weight percentage of each element of the alloy is an important factor affecting the crystal structure. The phase diagram of Co–Ni alloys suggests that incorporation of Ni in the Co lattice at room temperature may result in cubic phase if Ni content is greater than 30% (wt %).[19] Myung and Kobe[20] obtained face-centered-cubic Co–Ni when Co is kept below 70% as its phase diagram suggests.[20] Co–Ni–Mn–P films are expected to show a similar behavior since Mn and P contents are kept below a few percent.

The Ni content in the film can be increased by reducing the concentration of Co ions in the electrodeposition bath. When equal concentrations of $NiCl_2\cdot6H_2O$ and $CoCl_2\cdot6H_2O$ were used, it was measured that Co concentration in the film reaches 86%, whereas Ni concentration remains at 12%. Although deposition rate of pure Ni is greater than pure Co, when they are codeposited, Co deposits faster than Ni (anomalous codeposition).

The dependence of the film's Ni content on the $CoCl_2\cdot6H_2O$ dissolved in the bath was experimentally determined by a number of electrodepositions. The current density was set to 6 mA/cm^2 and deposition was done for 3 h for each film. Constant nitrogen agitation was applied during depositions. The results in Fig. 1 demonstrate that a Ni content of 30% or higher can be obtained if $CoCl_2.6H_2O$ concentration in the bath is kept below 11 g/l.

The thickness of the films was measured to be approximately 10 μm. High film thickness facilitates the crystallinity measurements by reducing the background noise caused by the substrate. Therefore, it is critical to have high thickness in order to obtain better XRD results. In addition, high film thickness increases the stored magnetic energy by increasing the film volume. High stored magnetic energy, therefore high force, is an important requirement for most applications of Co–Ni–Mn–P magnetic films.

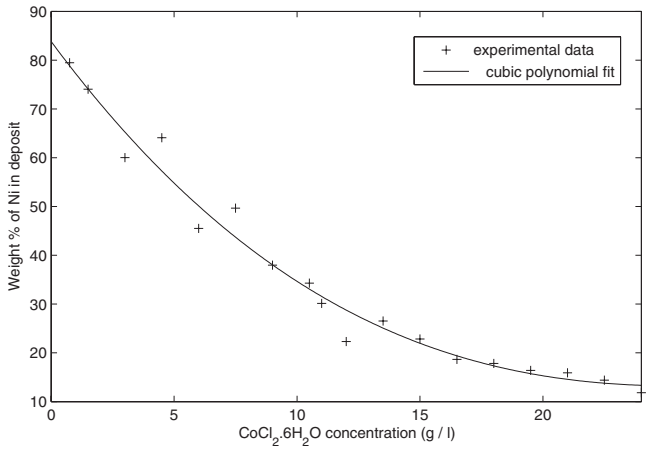

FIG. 1. Varying film Ni content.

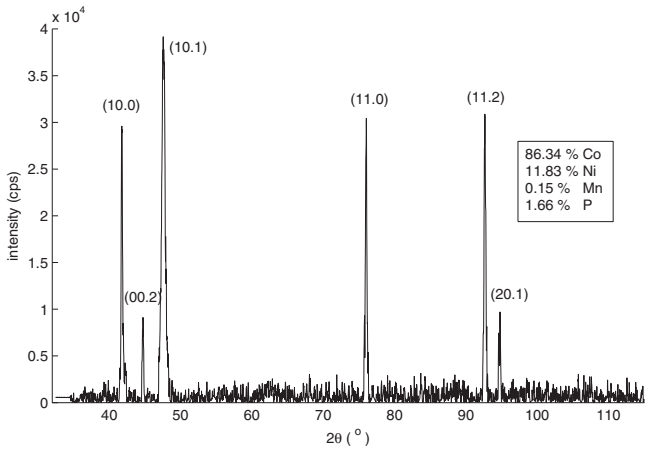

FIG. 2. XRD pattern of the film with low Ni content. (hcp diffraction peaks)

B. XRD measurements

Crystal structures of various concentrations of Co–Ni–Mn–P films deposited at a current density of 6 mA/cm^2 were studied using XRD. It is known that the electrodeposition kinetics are greatly influenced by the current density and agitation. To obtain crystalline thin films, a series of experiments was performed with varying current density and nitrogen agitation. It was observed that the depositions with low current density and no agitation resulted in better crystallization.

Previously, it was stated that reduced current density increases grain size and crystallinity.[14,21] Similarly, our results showed that crystallinity is promoted by low current density. It might be mainly because low current density reduces hydrogen evolution and induces smaller stress. Therefore, less discontinuity is formed in the film structure resulting in a highly crystallized structure.[22]

In order to investigate the effect of crystal structure on the magnetic properties of Co–Ni–Mn–P thin films, two samples were selected. The deposition parameters and the elemental compositions of the low Ni and high Ni films were summarized in Table II. Figure 2 illustrates the XRD pattern of the first film with a Ni content of 11.83%. The experimental and calculated diffraction data are compared in Table III. It is seen that the Co–Ni–Mn–P alloy forms a hexagonal-closed-pack (hcp) structure with preferably (10.1) texture.

When $CoCl_2.6H_2O$ concentration in the bath was decreased to 10.5 g/l, an alloy with 30.14% Ni was obtained. XRD measurements of this Ni-rich film (Fig. 3, Table IV) clearly illustrate the attenuation of hcp peaks and appearance of diamond cubic phase peaks.

Any peaks due to the crystalline substrate were hindered by depositing layers with large thicknesses (10 μm). Therefore, the demonstrated XRD data belong to the deposited film only and can easily be interpreted. Also, any effects of the substrate on the film structure were suppressed by growing films thicker than the substrate-dependent initial growth thickness.

It has been observed that by varying cobalt chloride concentration in the electrolyte, two types of crystal formations can be obtained for Co–Ni–Mn–P films. Increasing the Ni content in the deposit around 30% suppresses the hcp phase and forms a cubic structure. Since interatomic distance changes with a hcp to cubic transformation, the exchange interaction is greatly varied. This should lead to a profound change in the magnetic properties of the alloy.

The morphological difference between samples with hexagonal and cubic crystal structures is shown by cross-sectional SEM measurements. Figures 4 and 5, respectively, illustrate the grain structures for both films. The hexagonal film demonstrates slightly tilted columnar grains along film thickness (Fig. 4). On the other hand, cubic sample does not show a preferred grain orientation (Fig. 5).

C. Magnetic property measurements

The magnetic properties of the hexagonal and cubic films were determined by in-plane (horizontal) and out-of-plane (perpendicular to the film surface) hysteresis loop measurements at room temperature. Magnetic properties including coercive field (H_c), remanent field (B_r), and maximum energy product (BH_{max}) are listed in Table V. Maximum energy product values are calculated from the second quadrant of the hysteresis loops.

As can be seen in Table V, hexagonal films outperform cubic films in terms of perpendicular magnetization properties, whereas cubic films have superior horizontal magnetization characteristics. For instance, out-of-plane BH_{max} in-

TABLE II. Properties of selected samples.

	Elemental composition (wt %)				Deposition conditions	
	Co	Ni	Mn	P	Current density (mA/cm^2)	Duration (h)
Low Ni	86.34	11.83	0.15	1.66	4	4.5
High Ni	67.07	30.14	0.2	2.59	3	6

TABLE III. Experimental and calculated XRD values of Ni-poor film. $a_{Co}=2.507$ Å, $c_{Co}=4.07$ Å, and $d^{-1}=\sqrt{\frac{4(h^2+k^2+hk)}{3a^2}+\frac{l^2}{c^2}}$.

2θ (deg)	d_{exp} (Å)	d_{cal} (Å)	I (%)	(hkl)
41.76	2.161	2.171	75.6	(10.0)
44.72	2.025	2.035	23.3	(00.2)
47.56	1.910	1.916	100.0	(10.1)
76.04	1.251	1.254	77.7	(11.0)
92.66	1.065	1.067	78.8	(11.2)
94.78	1.047	1.049	24.8	(20.1)

creases up to 70% on average with a cubic to hexagonal transformation and in-plane BH_{max} triples for cubic films compared to hexagonal films.

The promoted out-of-plane magnetization of hexagonal films can be attributed to the fact that magnetocrystalline anisotropy of hexagonal Co is much higher than cubic Co.[17] When [0001] axis of the films (c-axis) coincides with the normal of the film surface, perpendicular magnetization is improved. In addition, the perpendicularly oriented grain structures of hexagonal films observed in Fig. 4 promote shape anisotropy. Resultantly, magnetocrystalline anisotropy and shape anisotropy reinforce each other in hcp films that leads to better out-of-plane magnetic properties.

It should be noted that magnetic properties of both hexagonal and cubic Co–Ni–Mn–P films are not as strong as rare-earth magnets (NdFeB and SmCo). However, electrodeposited Co–Ni–Mn–P films provide multidirectional magnetization and they are much inexpensive to produce. Therefore, they can be a good choice for disposable microsystems. In addition, as stated in previous studies, the magnetic properties listed in Table V can be improved by incorporating additional stress relievers to the solution,[14] applying magnetic field during deposition[13] or producing array structures instead of monolithic films.[15]

IV. APPLICATIONS

Magnetic thin films offer significant advantages in MEMS devices such as reduction in size, high stored energy, high force, and operation at room temperature. The most

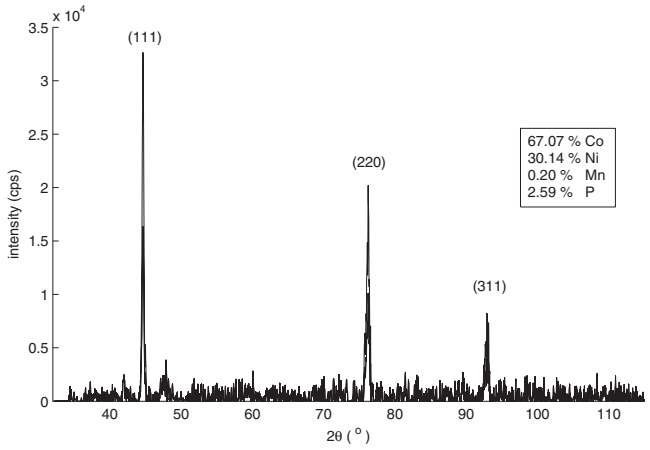

FIG. 3. XRD pattern of the film with high Ni content. (diamond cubic diffraction peaks)

TABLE IV. Experimental and calculated XRD values of Ni-rich film. $a_{Co-Ni}=3.537$ Å and $d=\frac{a}{\sqrt{h^2+k^2+l^2}}$.

2θ (deg)	d_{exp} (Å)	d_{cal} (Å)	I (%)	(hkl)
44.64	2.028	2.042	100.0	(111)
76.24	1.248	1.251	61.9	(220)
92.90	1.063	1.067	25.2	(311)

common applications of magnetic films in microsystems are giant magnetoresistive (GMR) sensors, bidirectional (push-pull) microactuators, and plastic deformation magnetic assembly (PDMA). These applications require either in-plane or out-of-plane magnetized films depending on the device design.

Vieux-Rochaz *et al.*[12] realized a GMR sensor using electrodeposited CoPtP magnetic films.[12] They have used the 5 μm thick films to bias the NiFe/Ag GMR elements.

Using magnetic thin films enables bidirectional actuation in microactuators that can be used in various devices. For instance, Taylor *et al.*[23] reported a microrelay using electroplated Permalloy thin film. Cugat *et al.*[24] demonstrated a micromirror magnetically actuated using sputtered NdFeB films with a thickness of 200 μm.[24] Gray *et al.*[25] fabricated a single pole double throw switch for rf MEMS applications. The microswitch employs a bidirectional microactuator made of electrodeposited Permalloy layer.[25]

Another application of magnetic thin films is PDMA, which is a technique to produce 3D structures in microscale.[26,27] In this technique, a magnetic thin film is deposited on a planar flap with flexible substrate connection. Then, external magnetic field is applied to the structure in the vertical direction. Due to the torque produced by the interaction of magnetic dipole moment of the magnetic film and the external field, the structure is deflected vertically. The external field is applied until the structure is plastically deformed at the flexure region. Using this method 3D self-standing microstructures can be produced.

It is worth mentioning that room temperature electrodeposition is compatible with other MEMS processing

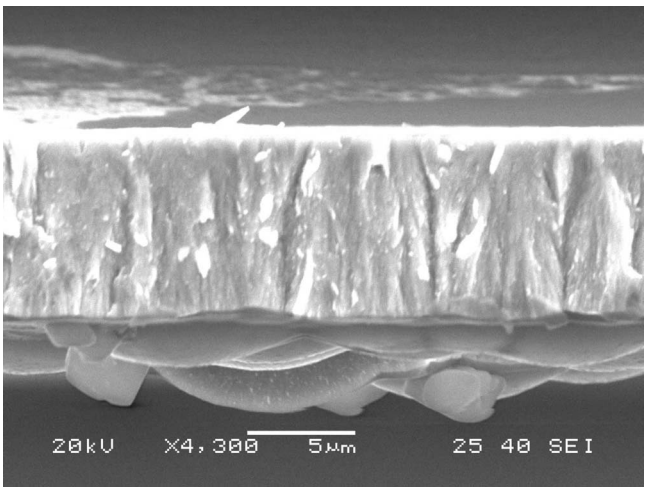

FIG. 4. Cross section of film with low Ni content.

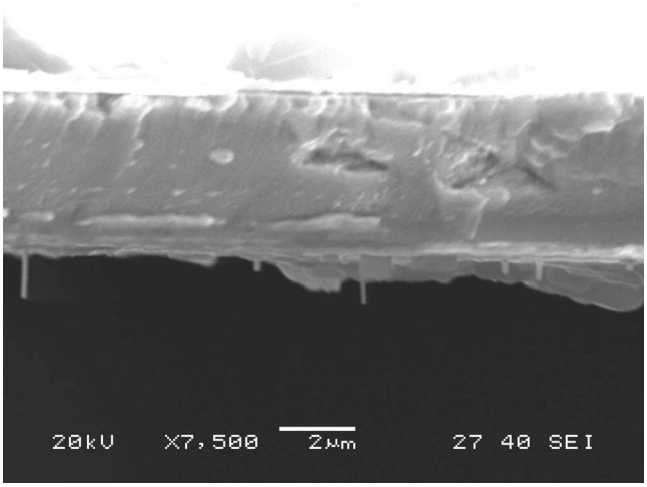

FIG. 5. Cross section of film with high Ni content.

techniques. Therefore, the magnetic film layers can be integrated into MEMS devices easily as seen in the above examples.

In this paper, we present a novel application for the magnetic thin films, which is magnetic levitation of microstructures. The main motivation behind this study is to eliminate the friction and adhesion forces during the positioning of MEMS. In addition, the operation will be completely dust-free and the device can be moved in a large working envelope without any wiring at all. As a first step in realizing such a system, the levitation of in-plane magnetized Co–Ni–Mn–P films is presented in the following sections.

A. Magnetic levitation setup

When a magnetic body is placed in an external field, the interaction between the magnetic dipole moment of the body and the external field applies a force to the body. This force can be calculated using Zeeman energy E_z, which can be expressed as

$$E_z = -\mu_0 \int_V \left(\frac{\mathbf{m}_0}{V} \cdot \mathbf{H} \right) dV, \tag{1}$$

where μ_0 is the absolute permeability, $\mathbf{m}_0$ is the dipole moment vector, and V is the volume of the magnetic body. $\mathbf{H}$ is the external magnetic field vector. When Zeeman energy is calculated for tiny objects, $\mathbf{H}$ is considered as constant through the volume of the object. Then Eq. (1) can be simplified as

TABLE V. Magnetic properties.

	Hexagonal films		Cubic films	
	In plane	Out of plane	In plane	Out of plane
B_r (kG)	1.4–1.6	0.5–0.7	1.6–2.3	0.3–0.5
H_c (Oe)	145–158	103–204	230–546	65–145
BH_{max} (kJ/m^3)	0.44–0.45	0.13–0.16	1.07–1.77	0.03–0.14

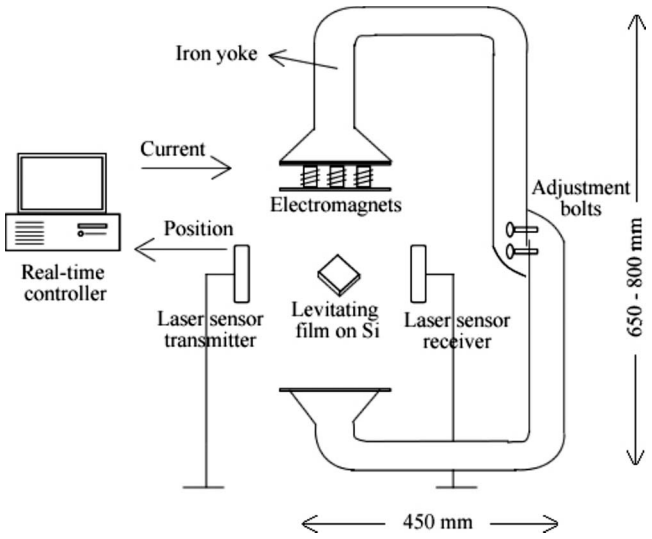

FIG. 6. Schematic of the magnetic levitation system.

$$E_z = -\mu_0 \cdot \frac{\mathbf{m}_0}{V} \cdot \mathbf{H} \cdot V = -\mathbf{m}_0 \cdot \mathbf{B}, \tag{2}$$

where $\mathbf{B}$ is the external magnetic flux density. Then, the levitation force can be found by taking the negative gradient of Zeeman energy as

$$\mathbf{F} = -\nabla E_z = \nabla(\mathbf{m}_0 \cdot \mathbf{B}). \tag{3}$$

In Cartesian coordinate system, the levitation force can be written as

$$\mathbf{F}_{\text{lev}} = \hat{x}\frac{\partial}{\partial x}(\mathbf{m}_0 \cdot \mathbf{B}) + \hat{y}\frac{\partial}{\partial y}(\mathbf{m}_0 \cdot \mathbf{B}) + \hat{z}\frac{\partial}{\partial z}(\mathbf{m}_0 \cdot \mathbf{B}). \tag{4}$$

Equation (4) suggests that the external field applies a force to the magnetic body in the direction of increasing magnetic flux density. Therefore, the magnetic levitation setup should generate a magnetic field such that the external magnetic field makes a single peak on the horizontal plane. When the levitating force balances the weight of the object, the object can be levitated at that peak magnetization point.

Our experimental setup generates the magnetic field using a magnetic drive unit composed of eight electromagnets, an iron yoke, and a laser displacement sensor. A schematic of the system is shown in Fig. 6. Feedback controller is used to adjust the magnetic field such that currents applied to the electromagnets are tuned to vary the levitation force and compensate for the weight of the levitating object. The details of the system can be found in another study of the authors where magnetic levitation of commercially available permanent magnets is described.[28] The magnetic flux density generated by the setup was measured with a Gaussmeter. Figure 7 demonstrates the planar magnetic flux density at a distance of 70 mm from the pole piece. It can be seen that the magnetic levitation setup can generate a magnetic field with a single $B_{\max}$ point on the plane. Therefore, the configuration illustrated in Fig. 6 is capable of levitating objects.

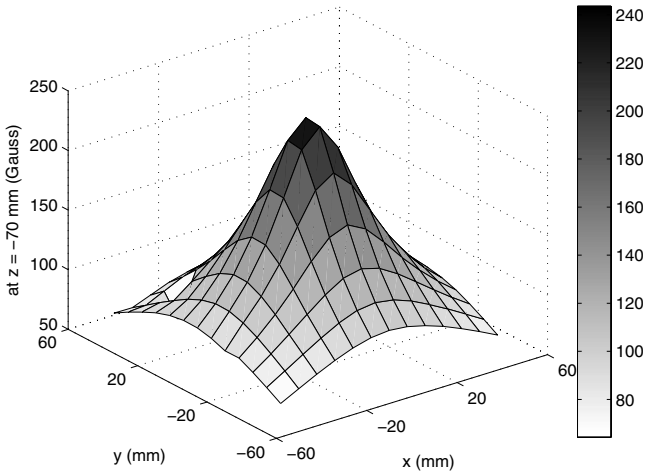

FIG. 7. Horizontal magnetic field generated by the levitation system.

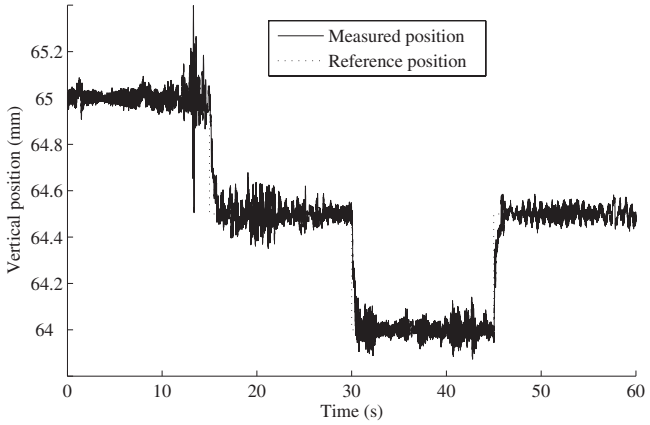

FIG. 9. Levitation of the Co–Ni–Mn–P film using step input.

B. Experimental results

The Co–Ni–Mn–P films were used to interact with external magnetic field and generate the levitation force. The handling and assembling of commercial micromagnets are tedious jobs and they also restrict the design of the device. However, when magnetic films are used, the designer has great flexibility in terms of the actual MEMS design. Magnetic levitation of the electrodeposited Co–Ni–Mn–P films demonstrates the capability of the system as shown in Fig. 6. The 5×5 mm^2 in-plane magnetized samples were tested for one-dimensional levitation. A step input trajectory was applied to move the magnetic film coated samples at a distance between 64 and 65 mm from the electromagnets. Due to in-plane magnetization, the film was levitated vertically along its surface diagonal as shown in Fig. 8. One of the electromagnets and the laser sensor receiver can also be seen in this figure. The position of the object was continuously recorded by the line-shape laser beam. Figure 9 shows the reference trajectory and the position of the object. The rms positioning error was calculated in Fig. 9 as 32.5 μm. These experiments verify that it is possible to control Co–Ni–Mn–P coated microdevices using the proposed system. Currently, the focus of the authors is to improve the precision of levitation by filtering out the noise and designing a better controller. This system has the potential to be used in microassembly and micromanipulation applications if an end effector is integrated into the levitated object such as a microgripper, a microprobe, or a microneedle.

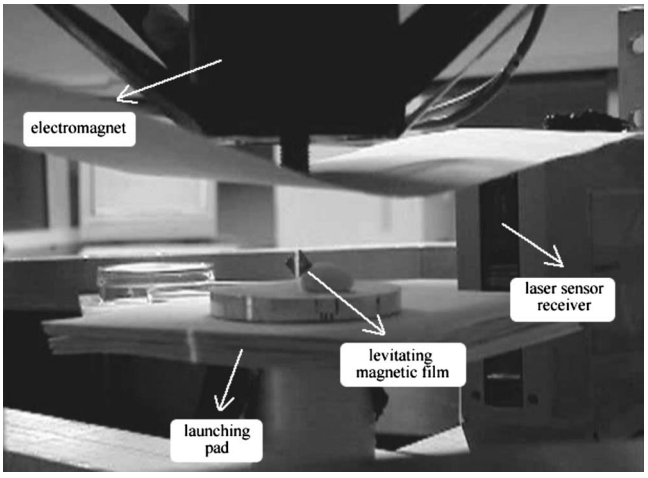

FIG. 8. The image of the levitating Co–Ni–Mn–P magnetic film.

V. CONCLUSION

In this work, a magnetic levitation system that is capable of levitating objects with micrometer precision was demonstrated. Crystalline Co–Ni–Mn–P films were produced for levitating microsystems. The crystal structure of the film has been found to play a decisive role in the direction of magnetization. Using the same fabrication technique, different crystal structures and magnetization in different directions were obtained. Although the magnetic properties of Co–Ni–Mn–P films are not as strong as rare-earth magnets, they provide magnetization in different directions and they are considerably more inexpensive. Silicon samples coated with horizontally magnetized Co–Ni–Mn–P films were levitated and moved in the vertical axis using a step trajectory. These results verify the idea of magnetic levitation of MEMS devices. As future work, a microgripper will be integrated into the levitating silicon sample for the handling of microparticles, hazardous materials, and biological samples. Biomanipulation and automated microassembly will be the potential applications of such a device.

[1]X. S. Wu, W. Y. Chen, X. L. Zhao, and W. P. Zhang, Electron. Lett. **40**, 996 (2004).
[2]M. Boukallel, J. Abadie, and E. Piat, 2003 IEEE International Conference on Robotics and Automation, Taipei, Taiwan, 2003 (unpublished), pp. 3219–3224.
[3]J. W. Jansen, C. M. M. van Lierop, E. A. Lomonova, and A. J. A. Vandenput, IEEE Trans. Magn. **43**, 15 (2007).
[4]E. Shameli, D. G. Craig, and M. B. Khamesee, J. Appl. Phys. **99**, 08P509 (2006).
[5]S. Kulkarni, S. Roy, T. O'Donnell, S. Beeby, and J. Tudor, J. Appl. Phys. **99**, 08P511 (2006).
[6]N. V. Myung, D. Y. Park, M. Schwartz, K. Nobe, H. Yang, C. K. Yang, and J. W. Judy, Proceedings of the Sixth International Symposium on Magnetic Materials, Processes and Devices, Pheonix, AZ, 2000 (unpublished), pp. 2000–2029.
[7]T. Osaka, N. Kasai, I. Koiwa, F. Gato, and Y. Suganuma, J. Electrochem. Soc. **130**, 568 (1983).
[8]S. Kulkarni and S. Roy, J. Appl. Phys. **101**, 09K524 (2007).
[9]H. Sato, T. Shimatsu, Y. Okazaki, H. Muraoka, H. Aoi, S. Okamoto, and O. Kitakami, J. Appl. Phys. **103**, 07E114 (2008).

[10]J. Horkans, D. J. Seagle, and I. H. Chang, J. Electrochem. Soc. **137**, 2056 (1990).
[11]Y. Su, H. Wang, G. Ding, F. Cui, W. Zhang, and W. Chen, IEEE Trans. Magn. **41**, 4380 (2005).
[12]L. Vieux-Rochaz, C. Dieppedale, B. Desloges, D. Gamet, C. Barragatti, H. Rostang, and J. Meunier-Carus, J. Micromech. Microeng. **16**, 219 (2006).
[13]H. J. Cho and C. H. Ahn, IEEE, Thirteenth Annual International Conference on Micro Electro Mechanical Systems, Piscataway, NJ, 2000 (unpublished), pp. 686–691.
[14]S. Guan and B. J. Nelson, J. Magn. Magn. Mater. **292**, 49 (2005).
[15]T. F. Liakopoulos, W. Zhang, and C. H. Ahn, IEEE, The Ninth Annual International Workshop on Micro Electro Mechanical Systems, San Diego, CA, 1996 (unpublished), pp. 79–84.
[16]W. B. Ng, A. Takada, and K. Okada, IEEE Trans. Magn. **41**, 3886 (2005).
[17]S. Armyanov, Electrochim. Acta **45**, 3323 (2000).
[18]H. J. Cho and C. H. Ahn, J. Microelectromech. Syst. **11**, 78 (2002).
[19]J. R. Davis, *ASM Specialty Handbook: Nickel, Cobalt, and their Alloys* (ASM International, Materials Park, OH, 2000), p. 352.
[20]N. V. Myung and K. Nobe, J. Electrochem. Soc. **148**, C136 (2001).
[21]I. Zana, Ph.D. thesis, University of Alabama, 2003.
[22]W. Ruythooren, K. Attenborough, S. Beerten, P. Merken, J. Fransaer, E. Beyne, C. V. Hoof, J. D. Boek, and J. P. Celis, J. Microelectromech. Syst. **10**, 101 (2000).
[23]W. P. Taylor, O. Brand, and M. G. Allen, J. Microelectromech. Syst. **7**, 181 (1998).
[24]O. Cugat, S. Basrour, C. Divoux, P. Mounaix, and G. Reyne, Sens. Actuators, A **89**, 1 (2001).
[25]G. D. Gray Jr., E. M. Prophet, L. Zhu, and P. A. Kohl, Sens. Actuators, A **119**, 502 (2005).
[26]Y. W. Yi and C. Liu, J. Microelectromech. Syst. **8**, 10 (1999).
[27]J. Zou, J. Chen, C. Liu, and J. E. Schutt-Aine, J. Microelectromech. Syst. **10**, 302 (2001).
[28]C. Elbuken, M. B. Khamesee, and M. Yavuz, J. Phys. D **39**, 3932 (2006).